International Journal of Architectural, Civil and Construction Sciences
ISSN: 2415-1734
Vol:7, No:6, 2013

Elastic Failure of Web-Cracked Plate Girder

Sebastian B. Mendes

***Abstract*—**The presence of a vertical fatigue crack in the web of a plate girder subjected to pure bending influences the bending moment capacity of the girder. The growth of the crack may lead to premature elastic failure due to flange local yielding, flange local buckling, or web local buckling. Approximate expressions for the bending moment capacities corresponding to these failure modes were formulated. Finite element analyses were then used to validate the expressions. The expressions were employed to assess the effects of crack length on the capacity. Neglecting brittle fracture, tension buckling, and ductile failure modes, it was found that typical girders are governed by the capacity associated with flange local yielding as influenced by the crack. Concluding, a possible use of the capacity expressions in girder design was demonstrated.

***Keywords*—**Fatigue crack, flange yielding, flange buckling, web buckling.

I. Introduction

PLATE girders form an important part of typical slab-girder highway bridges and are regularly subjected to fatigue loading produced by the ongoing passage of vehicles across the bridge structure. Over time the fatigue loading may lead to the gradual physical deterioration and consequential reduction in strength of a plate girder. A plate girder loaded under predominantly bending stresses experiences the most damaging effects in regions under fluctuating tensile stresses. Inherent discontinuities and imperfections in the plate girder induce local tensile stress concentrations which may eventually initiate the growth of a vertical through-thickness edge-crack through the web plate [1-13] (see Fig. 1). The growth of the edge-crack may ultimately bring about the premature elastic failure of the plate girder [14-20].

Numerous studies have investigated the influence of through-thickness cracks on the strength and stability of plate-like specimens loaded under compression, tension, and shear [21-34]. Research concerning beam-like structures has largely focused upon the effects of large discontinuities such as slots and copings on the bending and shear strength [35-44]. Far less research has concentrated upon the effects of through-thickness cracks on the strength of plate girders [45, 46].

The presence of a vertical through-thickness edge-crack in the tension region of a web plate induces a local disturbance in the normal bending stress distribution. Specifically, the edge-crack serves to locally shift the neutral axis of the plate girder towards the compression flange, which is accompanied by a local increase of the compressive bending stresses in the compression region of the web plate and in the compression flange. This local increase of stresses may give rise to the premature initiation of various elastic failure modes including flange local yielding, flange local buckling, and web local buckling.

The goal of this research was to derive approximate expressions for the bending moment capacities of a web-cracked plate girder corresponding to local yielding of the compression flange and elastic local buckling of the compression flange and web plate. Finite element (FE) analyses were performed using the general FE software ABAQUS to validate the derived capacity expressions. The capacity expressions were then plotted as functions of edge-crack length for various trial plate girders.

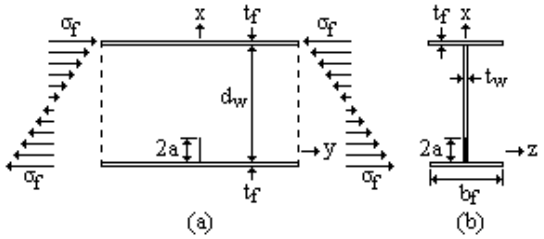

Fig. 1 (a) I-shaped plate girder loaded under pure bending and (b) section through edge-crack

II. Bending Stress Distribution

The normal bending stress distribution in uncracked sections of a plate girder is approximately described by classical beam theory in which the distribution takes on a linear form as shown in Fig. 2 (a). Using the coordinate system designated in Fig. 1, the linear bending stress distribution in any uncracked section is expressed as

$$\sigma_y = -\frac{2\sigma_w}{d_w}(x+a)+\sigma_w \tag{1}$$

where σ_w is the bending stress at the extreme fibers of the web plate, d_w is the depth of the web plate, and a is one half the edge-crack length.

S. B. Mendes is a Doctoral candidate at the Department of Civil and Environmental Engineering, University of Rhode Island, Kingston, RI 02881 USA (phone: 203-815-7640; e-mail: mendessb@my.uri.edu).

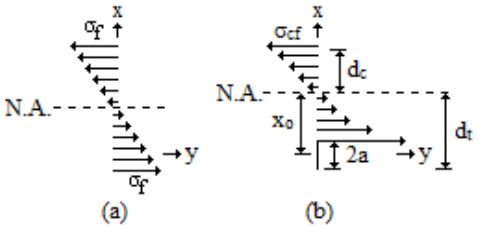

Fig. 2 (a) Normal bending stress distribution, σ_y, in uncracked section of a plate girder and (b) normal bending stress distribution, $\sigma_y(x,0)$, in cracked section

Given that plate girders are constructed of relatively thin plates, plane stress conditions are assumed to govern the stress field within the plates. The local disturbance in the web plate stress field induced by the edge-crack is approximately determined with the use of the Airy stress function, $F(x,y)$. The two-dimensional stress field for any elastic body may be expressed in terms of the Airy stress function as [47]

$$\sigma_x = \frac{\partial^2 F}{\partial y^2} \qquad \sigma_y = \frac{\partial^2 F}{\partial x^2} \qquad \tau_{xy} = -\frac{\partial^2 F}{\partial x \partial y} \tag{2}$$

where the Airy stress function satisfies the biharmonic equation given by [47]

$$\nabla^4 F = \frac{\partial^4 F}{\partial x^4} + 2\frac{\partial^4 F}{\partial x^2 \partial y^2} + \frac{\partial^4 F}{\partial y^4} = 0 \tag{3}$$

Hence satisfying the equilibrium and compatibility requirements. The presence of a crack within an elastic body requires an expanded definition of the stress field and is achieved by expressing the Airy stress function in terms of the Westergaard stress function, $Z(\zeta)$, as [48]

$$F = \mathrm{Re}\,\bar{\bar{Z}} + y\,\mathrm{Im}\,\bar{Z} \tag{4}$$

where

$$Z' = \frac{dZ}{d\zeta} \qquad Z = \frac{d\bar{Z}}{d\zeta} \qquad \bar{Z} = \frac{d\bar{\bar{Z}}}{d\zeta} \tag{5}$$

and ζ is the complex variable $\zeta = x + iy$. The substitution of (4) into (2) results in the stress field about a crack becoming

$$\begin{aligned} \sigma_x &= \mathrm{Re}\,Z - y\,\mathrm{Im}\,Z' \\ \sigma_y &= \mathrm{Re}\,Z + y\,\mathrm{Im}\,Z' \\ \tau_{xy} &= -y\,\mathrm{Re}\,Z' \end{aligned} \tag{6}$$

The normal bending stress distribution, $\sigma_y(x,0)$, along the x-axis (see Fig. 2 (b)) is approximated by assuming that the edge-crack resides within an infinite plate loaded by far-field stresses distributed identically to the uncracked bending stress distribution (see Fig 3 (a)) as expressed by (1). The stress field about the crack for this configuration is obtained by superimposing the stress fields for two distinct cases [49]. The first case consists of the infinite plate and far-field stresses without the crack. The second case consists of the crack within the infinite plate loaded by internal crack face stresses distributed identically to the uncracked bending stress distribution as expressed by (1). As a further simplification, the linearly varying crack face stresses are approximated as being uniformly distributed with a magnitude σ_w' taken as the average of the crack face stresses (see Fig. 3 (b)). This average stress is obtained by substituting $x = 0$ into (1) resulting in

$$\sigma_w' = -\frac{2\sigma_w a}{d_w} + \sigma_w \tag{7}$$

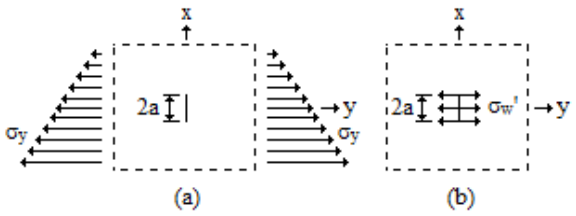

Fig. 3 (a) Infinite plate with central crack loaded by far-field stresses and (b) central crack within an infinite plate loaded by uniform crack face stresses

Superimposing the uncracked bending stress distribution for the first case as given by (1) with the stress distribution for the second case as given by $(6)_2$ and setting $y = 0$ results in

$$\sigma_y(x,0) = \mathrm{Re}\,Z + \sigma_y \tag{8}$$

The Westergaard stress function for the second case (see Fig. 3b) is given by [50, 51]

$$Z = \sigma_w'\left(\frac{\xi}{\sqrt{\xi^2 - a^2}} - 1\right) \tag{9}$$

Substituting (1) and (9) into (8) gives the final expression for the normal bending stress distribution along the x-axis

$$\begin{aligned} \sigma_y(x,0) = &\left(-\frac{2\sigma_w a}{d_w} + \sigma_w\right)\left(\frac{x}{\sqrt{x^2 - a^2}} - 1\right) \\ &-\frac{2\sigma_w}{d_w}(x + a) + \sigma_w \end{aligned} \tag{10}$$

The local shift of the neutral axis along the x-axis (see Fig. 2 (b)) is determined by equating (10) to zero and solving for x resulting in

$$x_o = \frac{1}{2}\sqrt{8a^2 - 4ad_w + d_w^2} \tag{11}$$

The depth of the web plate along the x-axis under tension, d_t, therefore becomes

$$d_t = x_o + a = \frac{1}{2}\sqrt{8a^2 - 4ad_w + d_w^2} + a \tag{12}$$

Also, the depth of the web plate along the x-axis under compression, d_c, becomes

$$d_c = d_w - d_t = d_w - a - \frac{1}{2}\sqrt{8a^2 - 4ad_w + d_w^2} \tag{13}$$

III. Local Yielding of Compression Flange

The localized shift of the neutral axis towards the compression flange increases the bending stresses in the compression flange along the x-axis which may lead to local yielding. For uncracked sections of a plate girder, the bending stresses at the extreme fibers of the compression flange, σ_f, and web plate, σ_w, are related by similar triangles in the form

$$\frac{\sigma_f}{d_w/2 + t_f} = \frac{\sigma_w}{d_w/2} \tag{14}$$

where t_f is the compression flange thickness. Solving for σ_w gives

$$\sigma_w = \frac{\sigma_f d_w}{d_w + 2t_f} \tag{15}$$

The local increase of bending stresses in the compression flange is first calculated by equating the compressive force in the uncracked section of the web plate with the compressive force in the cracked section of the web plate, expressed as

$$\frac{\sigma_w d_w t_w}{4} = \frac{\sigma_{cw} d_c t_w}{2} \tag{16}$$

where t_w is the web plate thickness and σ_{cw} is the increased bending stress at the extreme fibers of the web plate along the x-axis. Solving for σ_{cw} gives

$$\sigma_{cw} = \frac{\sigma_w d_w}{2d_c} \tag{17}$$

Assuming a linear distribution of compressive bending stresses above the shifted neutral axis along the x-axis, the increased bending stresses at the extreme fibers of the compression flange, σ_{cf}, is calculated by employing similar triangles in the form

$$\frac{\sigma_{cf}}{d_c + t_f} = \frac{\sigma_{cw}}{d_c} \tag{18}$$

for which solving for σ_{cf} results in

$$\sigma_{cf} = \frac{\sigma_{cw}\left(d_c + t_f\right)}{d_c} \tag{19}$$

Substituting (13) and (15) into (17) and introducing the result into (19) gives

$$\sigma_{cf} = \frac{\sigma_f}{\beta_{cf}} \tag{20}$$

where the factor β_{cf} is defined as

$$\beta_{cf} = \frac{\left(d_w + 2t_f\right)\left(2d_w - 2a - \sqrt{8a^2 - 4ad_w + d_w^2}\right)^2}{d_w^2\left(2t_f + 2d_w - 2a - \sqrt{8a^2 - 4ad_w + d_w^2}\right)} \tag{21}$$

Solving (20) for σ_f and setting σ_{cf} equal to the yield strength, σ_Y, of the girder material gives

$$\sigma_{f-cr} = \beta_{cf}\sigma_Y \le \sigma_Y \tag{22}$$

Equation (22) represents the critical bending stress at the extreme fibers of the compression flange in uncracked sections of a plate girder corresponding to yielding of the extreme fibers of the compression flange in the edge-cracked section along the x-axis. The bending moment capacity corresponding to local yielding of the compression flange is thus given by

$$M_{cr} = \sigma_{f-cr} S \tag{23}$$

where S is the elastic section modulus of the plate girder section with respect to the strong axis of bending.

IV. Elastic Local Buckling of Compression Flange

The local increase in bending stresses within the compression flange may alternatively lead to elastic local buckling of the compression flange stems. The critical bending stress at the extreme fibers of the compression flange in uncracked sections of a plate girder corresponding to elastic buckling of a flange stem in the edge-cracked section along the x-axis is determined using (20) and (21). Equating σ_{cf} in (20) to the classical elastic plate buckling capacity results in [52].

$$\sigma_{cf} = \sigma_{cr} = k\frac{D\pi^2}{t_f\left(b_f/2\right)^2} = \frac{\sigma_f}{\beta_{cf}} \tag{24}$$

where the factor k is dependent upon the geometrical properties and support conditions of the flange stem, and b_f is the compression flange width. D is the plate rigidity given by [52]

$$D = \frac{Et_f^3}{12(1-\nu^2)} \tag{25}$$

where E is the modulus of elasticity and v is Poisson's ratio. Substituting (25) into (24) and solving for σ_f gives

$$\sigma_{f-cr} = \beta_{cf}\sigma_{cr} = \beta_{cf}k\frac{\pi^2 E}{12(1-\nu^2)(b_f/2t_f)^2} \le \sigma_Y \tag{26}$$

One side of a flange stem is unrestrained while the side bordering the web plate is assumed to be simply supported or fully clamped. Assuming the restrained side to be fully clamped requires that $k = 4$ [52]. The bending moment capacity corresponding to elastic local buckling of the compression flange is thus given by

$$M_{cr} = \sigma_{f-cr}S \tag{27}$$

V. Elastic Local Buckling of Web Plate

The local increase in bending stresses within the compression region of the web plate influences the elastic web local buckling capacity of a plate girder. This capacity is estimated by first calculating the critical bending stress at the extreme fibers of the web plate, σ_{cw}, along the x-axis. A predefined region of the cracked web plate is assumed to locally buckle and the Rayleigh-Ritz method is employed to estimate σ_{cw}.

The predefined buckled region is presumed to be a square embedded plate of width d_c (see Fig. 4 (a)). This assumption is judged to be reasonable in light of the buckled shapes of cracked plates under tension obtained by Brighenti [24-26]. The central axis of the plate is aligned with the edge-crack along the x-axis. The plate is assumed to buckle in a form described by a shape function, $w(x,y)$. The edges of the plate are fully clamped, of which the boundary conditions are expressed as follows

$$\begin{aligned} &w(x_o,y)=0 \quad && w(x_o+d_c,y)=0 \\ &w(x,-d_c/2)=0 \quad && w(x,d_c/2)=0 \\ &\frac{w(x_o,y)}{dx}=0 \quad && \frac{w(x_o+d_c,y)}{dx}=0 \\ &\frac{w(x,-d_c/2)}{dy}=0 \quad && \frac{w(x,d_c/2)}{dy}=0 \end{aligned} \tag{28}$$

A shape function of the following form satisfies these boundary conditions

$$w(x,y) = A\left(\cos\frac{2\pi y}{d_c}\cos\frac{2\pi(x-x_o)}{d_c} - \cos\frac{2\pi y}{d_c} + \cos\frac{2\pi(x-x_o)}{d_c} - 1\right) \tag{29}$$

where A is an arbitrary variable subject to variation. The actual compressive bending stresses in the region above the edge-crack are approximated by loading the vertical sides of the embedded plate with the linear compressive bending stress distribution along the x-axis, $\sigma_y^c(x,0)$, as shown in Fig. 4 (b) and given by

$$\sigma_y^c(x,0) = \frac{\sigma_{cw}}{d_c}(x_o - x) \tag{30}$$

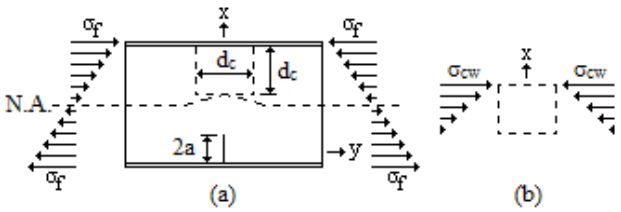

Fig. 4 (a) Location of embedded plate within the web plate and (b) the assumed external load distribution

The total potential energy, Π, of the loaded embedded plate is expressed as [53]

$$\Pi = \int_V W\,dV - \int_S T_i u_i\,dS = \frac{D}{2}\int_{-d_c/2}^{d_c/2}\int_{x_o}^{x_o+d_c}\left\{\left(\frac{\partial^2 w}{\partial x^2}+\frac{\partial^2 w}{\partial y^2}\right)^2 - 2(1-\nu)\left[\left(\frac{\partial^2 w}{\partial x^2}\right)\left(\frac{\partial^2 w}{\partial y^2}\right)-\left(\frac{\partial^2 w}{\partial x\partial y}\right)^2\right]\right\}dxdy + \frac{1}{2}\int_{-d_c/2}^{d_c/2}\int_{x_o}^{x_o+d_c}\left[\sigma_y^c(x,0)-\frac{d_c}{2}\right]\left(\frac{\partial w}{\partial x}\right)^2 dxdy \tag{31}$$

where W is the strain-energy density function, V is the volume of the plate, T_i are the applied surface tractions, u_i are the corresponding displacements, and S is the surface over which the tractions are applied. The y-intercept of (30) is shifted by a magnitude of $-d_c/2$ such that (30) is applied upon the vertical side of the embedded plate at $y = -d_c/2$. The change in total potential energy, $\delta\Pi$, with respect to A is then equated to zero. Solving for σ_{cw} and dividing the result by t_w gives

$$\sigma_{cw} = \frac{64D\pi^2 - 3d_c^3}{3t_w d_c^2} \tag{32}$$

The substitution of (13) and (15) into (17) gives

$$\sigma_{cw} = \frac{\sigma_f}{\beta_{cw}} \tag{33}$$

where the factor β_{cw} is defined as

$$\beta_{cw} = \frac{\left(d_w + 2t_f\right)\left(2d_w - 2a - \sqrt{8a^2 - 4ad_w + d_w^2}\right)}{d_w^2} \tag{34}$$

Introducing (32) into (33) and solving for σ_f results in

$$\sigma_{f-cr} = \beta_{cw} \frac{\left(64D\pi^2 - 3d_c^3\right)}{3t_w d_c^2} \le \sigma_Y \tag{35}$$

where t_w is used in place of t_f in the plate rigidity. It follows that the bending moment capacity corresponding to elastic local web buckling is given by

$$M_{cr} = \sigma_{f-cr} S \tag{36}$$

VI. FE Analyses

FE analyses were performed to validate the bending moment capacity expressions given by (23), (27), and (36). Four full-scale trial plate girders as well as corresponding full-scale trial web plates were modeled using ABAQUS. Each girder had a length, $L = 5\ m$, and was configured as a cantilever (see Fig. 5). The web plate depth was set to 127 cm and the flange plate width was set to 35 cm. The flange plate thickness was set as twice the thickness of the web plate thickness (see Table I). Also, each girder was modeled with the general material properties of alloy steel (modulus of elasticity, $E = 200\ GPa$; yield strength, $\sigma_Y = 345\ MPa$; Poisson's ratio, $v = 0.3$). An external bending moment, M_o, was applied to the free end of each girder such that the internal bending moment was constant throughout the length. Finally, each girder was modeled with four different through-thickness edge-crack lengths in the tension region of the web plate at mid-span (see Table I).

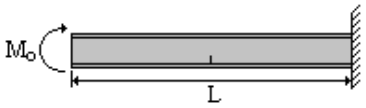

Fig. 5 Trial plate girder cantilever configuration

The web and flange plate thicknesses of PG-1 and PG-2 were purely theoretical for the purpose of investigating a broader spectrum of possible failure modes. The trial plate girders were meshed using 10-node quadratic tetrahedron solid elements. The entire face of one end of each girder was configured to have fully clamped support conditions. The external bending moment was modeled by loading the opposite face with a linearly varying normal stress distribution such that the top half was in compression and the bottom half in tension. The crack itself was modeled as a thin 0.1 cm wide extrusion through the web plate. A series of partitions were modeled about the crack to enable a finer mesh in the vicinity of the crack.

TABLE I
Trial Plate Girder Geometric Properties

Plate Girder (PG)	Web Thickness, t_w (cm)	Crack Length, 2a (cm)	Plate Girder (PG)	Web Thickness, t_w (cm)	Crack Length, 2a (cm)
PG-1a	0.15	6.0	PG-3a	0.60	6.0
PG-1b	0.15	12	PG-3b	0.60	12
PG-1c	0.15	24	PG-3c	0.60	24
PG-1d	0.15	48	PG-3d	0.60	48
PG-2a	0.30	6.0	PG-4a	1.20	6.0
PG-2b	0.30	12	PG-4b	1.20	12
PG-2c	0.30	24	PG-4c	1.20	24
PG-2d	0.30	48	PG-4d	1.20	48

The expressions for the normal bending stress distribution between the edge-crack tip and the shifted neutral axis given by (10), and between the shifted neutral axis and the extreme fibers of the compression flange given by (30), were first validated by employing PG-1 through PG-4. The external bending moment was set to $M_o = 500\ kN{\cdot}m$ and the corresponding bending stress distribution above the edge crack was numerically calculated. The plots of bending stress distributions for each girder and crack length as obtained from (10) and (30) as well as from the FE analyses are shown in Fig. 6.

Given that the analytical bending stress distributions closely correlated to the numerical results, PG-1 through PG-4 were next employed to validate the expression for the bending moment capacity corresponding to flange local yielding given by (23). This was achieved by increasing M_o to a magnitude exceeding the yield moment, M_y, and requesting stress history outputs of elements at the extreme outer fibers of the compression flange above the edge-crack. The bending moment at which the stresses in these elements exceeded the yield strength was then calculated. The capacities for each girder and crack length as calculated from (23) as well as from the FE analyses are listed in Table II. It is observed that a close correlation exists between the two sets of results.

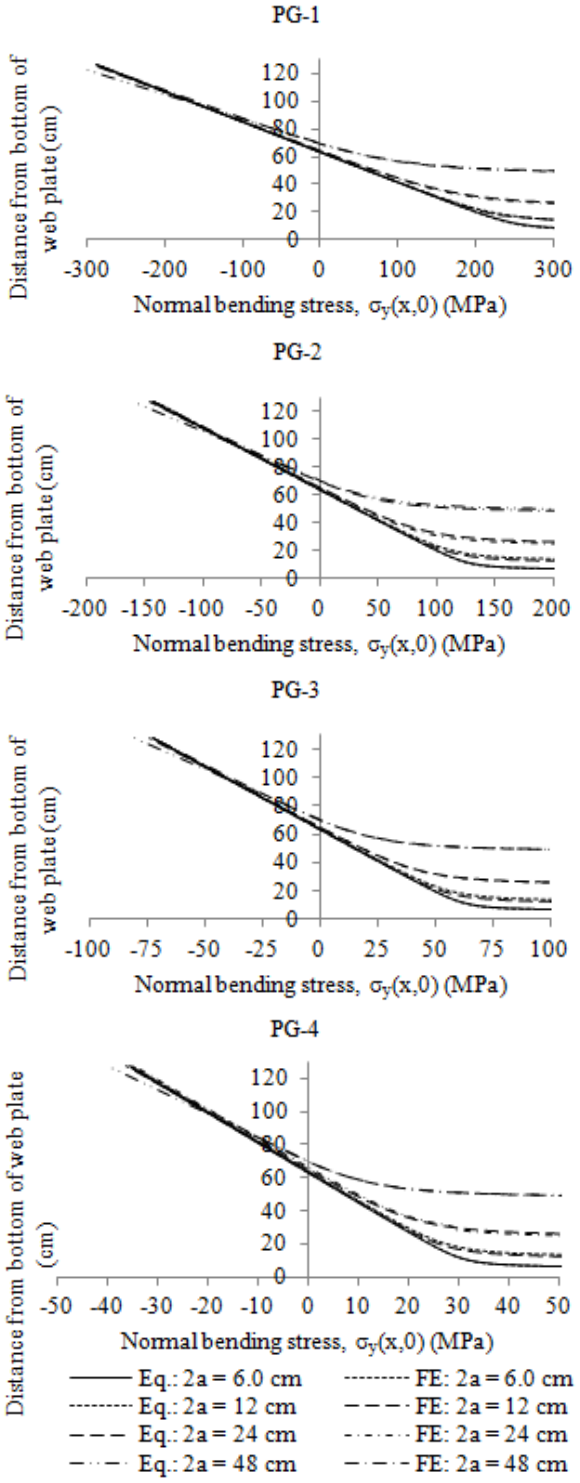

Fig. 6 Analytical and numerical normal bending stress distributions along the x-axis above the edge-crack for each trial plate girder

TABLE II
ANALYTICAL AND NUMERICAL FLANGE LOCAL YIELDING CAPACITIES

Plate Girder (PG)	Eq. (23) (kN·m)	FE (kN·m)	Error (%)	Plate Girder (PG)	Eq. (23) (kN·m)	FE (kN·m)	Error (%)
PG-1a	597.9	598.6	-0.10	PG-3a	2384	2386	-0.08
PG-1b	595.6	598.6	-0.50	PG-3b	2374	2386	-0.50
PG-1c	585.5	596.6	-1.86	PG-3c	2334	2386	-2.18
PG-1d	534.9	595.7	-10.2	PG-3d	2129	2380	-10.5
PG-2a	1194	1196	-0.17	PG-4a	4749	4754	-0.10
PG-2b	1190	1196	-0.50	PG-4b	4730	4754	-0.50
PG-2c	1170	1193	-1.92	PG-4c	4647	4754	-2.25
PG-2d	1068	1192	-10.4	PG-4d	4233	4752	-10.9

The numerical buckling simulations employed by the FE analyses are made difficult in part by global and local buckling modes overriding intended buckling modes. The expression for the bending moment capacity corresponding to flange local buckling given by (27) was indirectly validated by recognizing that the accuracy of (27) is directly dependent upon the accuracy of the stress at the extreme fibers of the compression flange as well as the accuracy of the bending stress distribution given by (10) and (30). The close correlation between the analytical and numerical bending moment capacities associated with flange local yielding signified that the corresponding critical stresses at the extreme fibers of the compression flange also exhibited a close correlation. Furthermore, given that (10) and (30) were previously validated, it was judged that (27) represents a reasonably accurate expression of the bending moment capacity associated with flange local buckling.

Full-scale trial web plates corresponding to PG-1 through PG-4 were employed to indirectly validate the expression for the bending moment capacity corresponding to web local buckling given by (36). Only the web plates were modeled in order to avoid the aforementioned difficulties concerning numerical buckling simulations. Each web plate was configured to have fully clamped support conditions along the longitudinal edges bordering the flange plates. The web plates were modeled using 4-node shell elements. The associated edge-cracks were modeled by assigning a seam to a single-line partition. Furthermore, the out-of-plane translation of each web plate was restrained except for the region of the embedded plate, thus reducing the analysis to that of a fully clamped embedded plate.

The vertical sides of the embedded plate were then loaded with a unit compressive stress distribution in the form expressed by (30). The first buckling mode stress corresponding to σ_{cw} was then computed and introduced into (33). The bending moment capacity was then calculated by solving (33) for σ_f and plugging the result into (36). The capacities for each girder and crack length as calculated from (36) as well as from the FE analyses are listed in Table III. It can be seen that the analytical and numerical results exhibit rough uniformity. The correlation is much more accurate for

very thin web plates (PG-1 and PG-2). A substantial amount of accuracy is lost for thicker web plates, thus signifying the possible need for further experimental analyses and correction factors.

TABLE III
ANALYTICAL AND NUMERICAL WEB LOCAL BUCKLING CAPACITIES

Plate Girder (PG)	Eq. (36) (kN·m)	FE (kN·m)	Error (%)	Plate Girder (PG)	Eq. (36) (kN·m)	FE (kN·m)	Error (%)
PG-1a	30.2	27.9	8.24	PG-3a	2422	1780	36.1
PG-1b	30.4	28.1	8.19	PG-3b	2431	1784	36.3
PG-1c	31.3	28.5	9.82	PG-3c	2473	1825	35.5
PG-1d	36.0	35.2	2.27	PG-3d	2708	1994	35.8
PG-2a	294.1	223.2	31.8	PG-4a	19711	14106	39.7
PG-2b	295.3	224.6	31.5	PG-4b	19786	14144	39.9
PG-2c	300.7	227.9	31.9	PG-4c	20126	14602	37.8
PG-2d	330.9	249.0	32.9	PG-4d	22021	15936	38.2

VII. RESULTS AND DISCUSSION

Having validated the capacity expressions, (23), (27), and (36) were plotted as functions of edge-crack length for each trial plate girder (see Fig. 7). The horizontal segments of the plots indicate the yield moment capacity. Web local buckling is the governing failure mode for PG-1 and PG-2. This is reflective of the extremely thin web plate thicknesses. It can be seen that the web local buckling capacity gradually increases with increasing crack length. This phenomenon was previously observed by Brighenti [24-26] and Khedmati et al. [27] in numerical tests of centrally cracked plates under compression. The increase in buckling strength despite the local increase in bending stresses is in part explained by the shrinking of the embedded plate as the crack length increases.

Flange local yielding is the governing failure mode for the realistic trial plate girders (PG-3 and PG-4). It is observed that the crack must grow to a length in the order of 20 - 25 cm before the elastic bending moment capacity begins to significantly decrease. For instance, a crack length of $2a = 5$ *cm* results in a negligible decrease in capacity relative to M_y, while a crack length of $2a = 40$ *cm* results in a decrease of 7%. Two criteria must then be met in order for premature flange local yielding failure to occur in this particular type of cracked section. First, the crack length must be within or exceed the range of 20 - 25 cm. Second, the required elastic bending moment capacity, M_r, must be just below the provided capacity, M_{cr}.

A simplified example of a possible use of the capacity expressions is as follows. A plate girder being designed for predominantly bending stresses must have a required elastic bending moment capacity of $M_r = 2250$ *kN·m*. Sizing the girder with the dimensions of PG-3 results in an elastic capacity of $M_{cr} = M_y = 2386$ *kN·m*. Since $M_r < M_{cr} = M_y$, the elastic capacity is satisfied. However, designing for a presumed edge-crack in the web plate with $2a = 40$ *cm* results in an elastic capacity governed by flange local yielding of

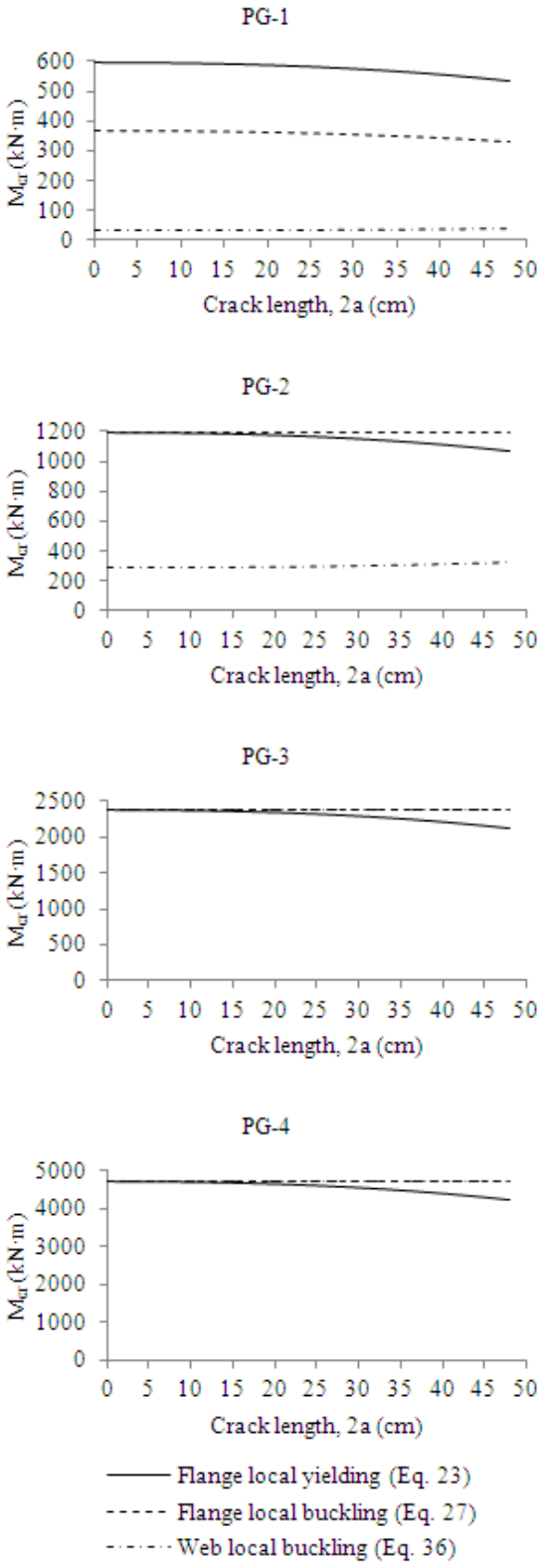

Fig. 7 Plots of bending moment capacity expressions as functions of edge-crack length for each trial plate girder

$M_{cr} = 2219\ kN{\cdot}m$. In this case, $M_r > M_{cr}$ and the girder section must be enlarged. Resizing the girder with the dimensions of PG-4 results in an elastic capacity of $M_{cr} = 4415\ kN{\cdot}m$ when $2a = 40\ cm$, thus satisfying the strength requirement. The section dimensions may be fine tuned to attain greater efficiency.

Additional elastic failure modes including web local buckling due to transverse compressive stresses adjacent to the edge-crack, brittle fracture, and a critical plastic zone size at the crack tip were not investigated in this particular study. However, these alternative failure modes may indeed govern depending upon the plate girder dimensions and load requirements.

REFERENCES

[1] Kouba, N.G., and Stallmeyer, J.E., "The behavior of stiffened beams under repeated loads," University of Illinois, Urbana, IL, Structural Research Series No. 173, 1959.
[2] Yen, B.T., "On the fatigue strength of welded plate girders," Lehigh University, Bethlehem, PA, Fritz Eng. Lab. Rep. No. 303-1, 1963.
[3] Hall, L.R., and Stallmeyer, J.E., "Thin web girder fatigue behavior as influenced by boundary rigidity," University of Illinois, Urbana, IL, Structural Research Series No. 278, 1964.
[4] Goodpasture, D.W., and Stallmeyer, J.E., "Fatigue behavior of welded thin web girders as influenced by web distortion and boundary rigidity," University of Illinois, Urbana, IL, Structural Research Series No. 328, 1967.
[5] Yen, B.T., and Mueller, J.A., "Fatigue tests of large-size welded plate girders," Lehigh University, Bethlehem, PA, Fritz Eng. Lab. Rep. No. 303-10, 1966.
[6] Mueller, J.A., and Yen, B.T., "Girder web boundary stresses and fatigue," Lehigh University, Bethlehem, PA, Fritz Eng. Lab. Rep. No. 327-2, 1967.
[7] Davies, A.W., Roberts, T.M., Evans, H.R., and Bennett, R.J.H., "Fatigue of slender web plates subjected to combined membrane and secondary bending stresses," *J. Construct. Steel Research,* vol. 30, no. 1, pp. 85-101, 1994.
[8] Roberts, T.M., Davies, A.W., and Bennett, R.J.H., "Fatigue shear strength of slender web plates," *J. Struct. Eng.*, vol. 121, no. 10, pp. 1396-1401, 1995.
[9] Crocetti, R., "Web breathing of full-scale slender I-girders subjected to combined action of bending and shear," *J. Construct. Steel Research,* vol. 59, no. 3, pp. 271-290, 2003.
[10] Marek, P., Perlman, M., Pense, A.W., and Tall, L., "Fatigue tests on a welded beam with pre-existing cracks," Lehigh University, Bethlehem, PA, Fritz Eng. Lab. Rep. No. 358-4A, 1970.
[11] Lawn, B., *Fracture of Brittle Solids*, 2nd ed. E.A. Davis, and I.M. Ward, Eds. Cambridge, UK: Cambridge University Press, 1993, ch. 9.
[12] Rolfe, S.T., and Barsom, J.M., *Fracture and Fatigue Control in Structures: Applications of Fracture Mechanics*. Englewood Cliffs, NJ: Prentice-Hall, 1977, ch. 7.
[13] Osman, M.H., and Roberts, T.M., "Prediction of the fatigue life of slender web plates using fracture mechanics concepts," *Thin-Walled Struct.*, vol. 35, no. 2, pp. 81-100, 1999.
[14] Kirke, B., and Al-Jamel, I.H., *Steel Structures Design Manual to AS 4100*. Author, 2004, sec. 2.3.3.
[15] Lichtenstein, *Special Inspections of Selected Portions of The Providence Viaduct, Route I-95 from West Exchange Street to Promenade Street, Bridge No. 578* (Supplemental Report for Project No. 1213). Framingham, MA: A.G. Lichtenstein and Associates, Inc, 1990.
[16] Minor, J., and Woodward, C., "Web buckle at I-40 bridge test," *J. Bridge Eng.*, vol. 1, no. 1, pp. 34-36, 1996.
[17] Chajes, M., Mertz, D., Quiel, S., Roecker, H., and Milius, J., "Steel girder fracture on Delaware's I-95 bridge over the Brandywine River," in *Proc. Structures Congress 2005*.
[18] Bowman, M.D., "Brittle fracture of the Blue River Bridge," in *Proc. Structures Congress 2004*.
[19] Zhou, Y.E., and Biegalski, A.E., "Investigation of large web fractures of welded steel plate girder bridge," *J. Bridge Eng.*, vol. 15, no. 4, pp. 373-383, 2010.
[20] Wardhana, K., and Hadipriono, F.C., "Analysis of recent bridge failures in the United States," *J. Performance of Constructed Facilities*, vol. 17, no. 3, pp. 144-150, 2003.
[21] Vafai, A., and Estekanchi, H.E., "A parametric finite element study of cracked plates and shells," *Thin-Walled Struct.,* vol. 33, no. 3, pp. 211-229, 1999.
[22] Kumar, Y.V.S., and Paik, J.K., "Buckling analysis of cracked plates using hierarchical trigonometric functions," *Thin-Walled Struct.,* vol. 42, no. 5, pp. 687-700, 2004.
[23] Paik, J.K., Kumar, Y.V.S., and Lee, J.M., "Ultimate strength of cracked plate elements under axial compression or tension," *Thin-Walled Struct.*, vol. 43, no. 2, pp. 237-272, 2005.
[24] Brighenti, R., "Buckling of cracked thin-plates under tension or compression," *Thin-Walled Struct.,* vol. 43, no. 2, pp. 209-224, 2005.
[25] Brighenti, R., "Numerical buckling analysis of compressed or tension cracked thin plates," *Eng. Struct.,* vol. 27, no. 2, pp. 265-276, 2005.
[26] Brighenti, R., "Buckling sensitivity analysis of cracked thin plates under membrane tension or compression loading," *Nuclear Eng. and Design,* vol. 239, no. 6, pp. 965-980, 2009.
[27] Khedmati, M.R., Edalat, P., and Javidruzi, M., "Sensitivity analysis of the elastic buckling of cracked plate elements under axial compression," *Thin-Walled Struct.*, vol. 47, no. 5, pp. 522-536, 2009.
[28] Seifi, R., and Khoda-yari, N., "Experimental and numerical studies on buckling of cracked thin-plates under full and partial compression edge loading," *Thin-Walled Struct.*, vol. 49, no. 12, pp. 1504-1516, 2011.
[29] Alinia, M.M., Hosseinzadeh, S.A.A., and Habashi, H.R., "Buckling and post-buckling strength of shear panels degraded by near border cracks," *J. Construct. Steel Research*, vol. 64, no. 12, pp. 1483-1494, 2007.
[30] Alinia, M.M., Hosseinzadeh, S.A.A., and Habashi, H.R., "Influence of central cracks on buckling and post-buckling behaviour of shear panels," *Thin-Walled Struct.*, vol. 45, no. 4, pp. 422-431, 2007.
[31] Alinia, M.M., Hosseinzadeh, S.A.A., and Habashi, H.R., "Numerical modelling for buckling analysis of cracked shear panels," *Thin-Walled Struct.*, vol. 45, no. 12, pp. 1058-1067, 2007.
[32] Brighenti, R., and Carpinteri, A., "Buckling and fracture behaviour of cracked thin plates under shear loading," *Materials and Design*, vol. 32, no. 3, pp. 1347-1355, 2011.
[33] Guz, A.N., and Dyshel, M.Sh., "Fracture and buckling of thin panels with edge crack in tension," *Theo. and Appl. Fract. Mech.,* vol. 36, no. 1, pp. 57-60, 2001.
[34] Guz, A.N., and Dyshel, M.Sh., "Stability and residual strength of panels with straight and curved cracks. *Theo. and Appl. Fract. Mech.,* vol. 31, nos. 1-3, pp. 95-101, 2004.
[35] Cooper, P.B., and Roychowdhury, J., "Shear strength of plate girders with web openings," *J. Struct. Eng.,* vol. 116, no. 7, pp. 2042-2048, 1990.
[36] Narayanan, R., and Der-Avanessian, N., "Design of slender webs having rectangular holes," *J. Struct. Eng.,* vol. 111, no. 4, pp. 777-787, 1985.
[37] Cheng, J., and Yura, J., "Local web buckling of coped beams," *J. Struct. Eng.*, vol. 112, no. 10, pp. 2314-2331, 1986.
[38] Ito, M., Fujiwara, K., and Okazaki, K., " Ultimate strength of beams with U-shaped holes in top of web," *J. Struct. Eng.,* vol. 117, no. 7, pp. 1929-1945, 1991.
[39] Zaarour, W., and Redwood, R., "Web buckling in thin webbed castellated beams," *J. Struct. Eng.,* vol. 122, no. 8, pp. 860-866, 1996.
[40] Redwood, R., and Demirdjian, S., "Castellated beam web buckling in shear," *J. Struct. Eng.*, vol. 124, no. 10, pp. 1202-1207, 1998.
[41] Shanmugam, N.E., Lian, V.T., and Thevendran, V., "Finite element modelling of plate girders with web openings," *Thin-Walled Struct.*, vol. 40, no. 5, pp. 443-464, 2002.
[42] Hagen, N.C., Larsen, P.K., and Aalberg, A., "Shear capacity of steel plate girders with large web openings, part I: Modeling and simulations," *J. Construct. Steel Research,* vol. 65, no. 1, pp. 142-150, 2009.
[43] Hagen, N.C., and Larsen, P.K., "Shear capacity of steel plate girders with large web openings part II: Design guidelines," *J. Construct. Steel Research*, vol. 65, no. 1, pp. 151-158, 2009.
[44] Bedair, O., "Stress analyses of deep plate girders used at oil and gas facilities with rectangular web penetrations," *Practice Periodical on Struct. Design and Construct.*, vol. 16, no. 3, pp. 112-120, 2011.

[45] Roberts, R., Fisher, J.W., Irwin, G.R., Boyer, K.D., Hausammann, G.V., Krishna, V., Morf, R., and Slockbower, R.E., "Determination of tolerable flaw sizes in full size welded bridge details," Lehigh University, Bethlehem, PA, Fritz Eng. Lab. Rep. No. 399-3, 1977.
[46] Roberts, T.M., Osman, M.H., Skaloud, M., and Zornerova, M., "Residual shear strength of fatigue cracked slender web panels," *Thin-Walled Struct.,* vol. 24, no. 2, pp. 157-172, 1996.
[47] Sadd, M.H., *Elasticity: Theory, Applications, and Numerics,* 2nd ed. Burlington, MA: Academic Press, 2009, sec. 7.5.
[48] Westergaard, H.M., "Bearing pressures and cracks," *J. Applied Mech.,* vol. 6, no. 61, pp. 49-53, 1939.
[49] Sun, C.T., and Jin, Z.-H., *Fracture Mechanics*. Waltham, MA: Academic Press, 2012, sec. 3.5.
[50] Sedov, L.I., *A Course in Continuum Mechanics*. J.R.M. Radok, Trans. Groningen, Netherlands: Wolters-Noordhoff Publishing, 1972, sec. 13.2.8.
[51] Fett, T., *Stress Intensity Factors, T-Stresses, Weight Functions*. Karlsruhe, Germany: Universitätsverlag Karlsruhe, 2008.
[52] Salmon, C.G., Johnson, J.E., and Malhas, F.A., *Steel Structures: Design and Behavior*, 5th ed. Upper Saddle River, NJ: Pearson Prentice Hall, 2009, secs. 6.14, 6.15.
[53] Vinson, J.R., *Structural Mechanics: The Behavior of Plates and Shells*. New York, NY: John Wiley & Sons, Inc., 1974, sec. 6.1.